# Effect of Nozzle Port Angle on Mold Surface Flow in Steel Slab Casting

Nozzle port angle is a critical parameter controlling fluid flow in the continuous casting mold, especially across the top surface. Fluid flow calculations with a three-dimensional (3D) k-ε model and die-injection experiments on a one-third-scale water model were performed to quantify the effects of nozzle angle on flow pattern and surface flow. The 15° up-angled nozzle produces more severe jet wobbling for the conditions simulated, resulting in velocity fluctuations at the surface. This could increase surface cracks, powder entrapment and associated downstream problems, especially in advanced high-strength steels.

## Authors

Seong-Mook Cho
postdoctoral research associate, Department of Mechanical Science and Engineering, University of Illinois at Urbana-Champaign, Urbana, Ill., USA
y104401@illinois.edu

Brian G. Thomas
professor, Department of Mechanical Engineering, Colorado School of Mines, Golden, Colo., USA
bgthomas@mines.edu

Hyoung-Jun Lee
senior researcher, steelmaking research group, POSCO Technical Research Laboratories, Pohang, Gyeongbuk, Republic of Korea

Seon-Hyo Kim
professor, Department of Materials Science and Engineering, Pohang University of Science and Technology, Pohang, Gyeongbuk, Republic of Korea

During the continuous casting of steel slabs, abnormal surface velocity, surface level and their fluctuations are major causes of surface quality problems in final rolled products. Surface-level fluctuations near the solidifying steel shell on the narrow faces (NF) and wide faces (WF) can entrap surface mold flux into the solidifying steel shell.[1–3] Excessive surface velocity increases shear instability at the liquid mold flux/molten steel interface, resulting in mold flux entrainment.[4–6] On the other hand, surface velocity that is too slow can produce low and non-uniform surface temperature, including meniscus freezing, hook formation[7,8] and surface defects related to initial solidification problems.

To control surface velocity and level, many efforts have been made to optimize nozzle port design and casting conditions, including gas injection and electromagnetic systems. Nozzle design is one of the most important process parameters that can be easily changed in the steel plant to optimize the surface velocity. Chaudhary et al. investigated the effect of nozzle bottom shapes (well- and mountain-type bottom) on surface velocity and its fluctuations.[9] They found that the mountain-type bottom produces higher velocity and more unstable flow and turbulence at the top surface, causing higher variations in the surface-level profile, level fluctuations, and easier slag entrainment, owing to its increased sensitivity to flow variations; thus the well bottom nozzle is better for steel quality. Najjar et al. investigated the effect of nozzle design (port angle, port dimensions (height, width, thickness), port side dispersion angle, port shape, bottom design, number of ports) on nozzle flow.[10] They found that deeper (more downward) angled nozzle ports produce deeper jet angle. This work applies both one-third-scale water model experiments and computational modeling of the water model to investigate the effect of nozzle port angle on not only nozzle flow, but also mold flow pattern, surface velocity and turbulence, for a different set of casting conditions.

## Methodology

**Water Model Experiment** — A one-third-scale water model of the real continuous caster, shown in Fig. 1, was used for experiments to measure nozzle and mold flow. The water model consists of a half-tundish, stopper rod, submerged-entry nozzle (SEN) and mold. The water flowrate from the tundish through the SEN into the mold is controlled by changing the size of the annular gap between the stopper and the bottom of the tundish. Water at 25°C exits holes in the mold bottom to a holding water bath and is pumped continuously back up to the tundish. Two different nozzle ports shown in Fig. 2 were investigated in this study of the effect of port angle on the mold surface flow. Both nozzles were bifurcated with typical rectangular ports with slightly rounded corners, differing only in the angle of the ports: +15° (up angle) or –15° (down angle) at both upper and lower edges. Table 1 provides details of the casting conditions, nozzle, and mold dimensions of the real caster and the one-third-scale water model. The casting speed was chosen based on

Figure 1

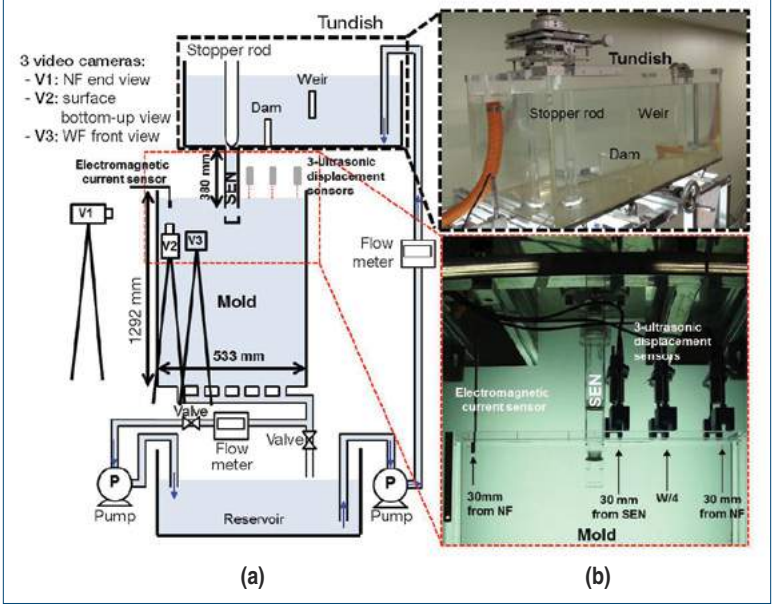


*Schematic (a) and photos (b) of one-third-scale water model.*

maintaining a constant Froude number, which is defined as the ratio of inertia force to gravitational force as follows:

$$\left(V_{Casting,W}/\sqrt{gL_W}\right)=\left(V_{Casting,R}/\sqrt{gL_R}\right) \quad \text{(Eq. 1)}$$

where

W = water model,
R = real caster,
$V_{casting}$ = casting speed,
L = scale length and
g = gravitational acceleration.

Rearranging this equation gives the casting speed in the water model, $V_{Casting,W}$, as follows:

$$V_{Casting,W}=V_{Casting,R}\sqrt{L_W/L_R} \quad \text{(Eq. 2)}$$

Measurements of instantaneous surface velocity were performed using an electromagnetic current sensor located at the three positions shown in Fig. 3: (1) 30 mm from narrow face (NF), (2) W/8, and (3) W/4 positions on the left NF and 10 mm from free surface in the water model (W = mold width). Instantaneous horizontal velocity data was collected for 1,000 seconds at 10 Hz. The sensor can measure two components of horizontal surface velocity: one parallel and the other perpendicular to the mold width direction. In addition, dye and a small amount (0.06% volume fraction of total volume flowrate of water and argon gas) of argon gas were injected to visualize the flow patterns. The visualized

Figure 2


*Nozzle ports: +15° (up angle) (a) and –15° (down angle) (b).*

Figure 3

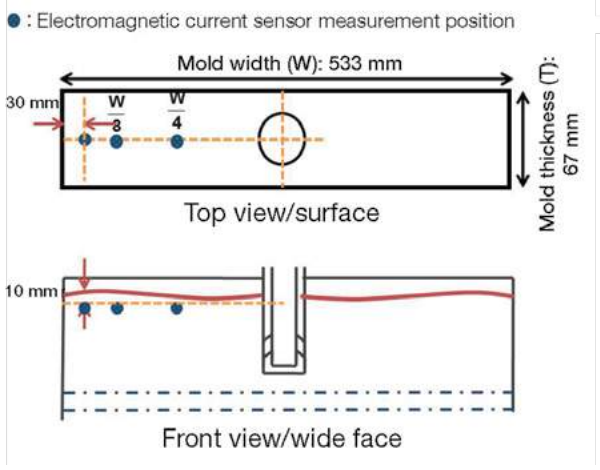


*Sensor positions for measurements.*

Table 1

*Caster Dimensions and Process Conditions*

| | Real caster (R) | One-third-scale water model (W) |
|---|---|---|
| Casting speed | $V_{Casting,R}$: 0.8 m/minute | $V_{Casting,W}$ : 0.5 m/minute |
| Volume flowrate | 256.0 lpm | 16.4 lpm |
| Submerged depth of nozzle | 140 mm | 46.7 mm |
| Mold width | 1600 mm | 533 mm |
| Mold thickness | 200 mm | 67 mm |
| Aspect ratio between mold width and thickness | 8.0 | |
| Nozzle port angle | +15° (up angle), -15° (down angle) | |
| Nozzle port size (width x height/radius of rounded corner) | 60 mm x 65 mm/20 mm | 20 mm x 21.7 mm/6.7 mm |
| Nozzle bore (inner/outer) | ∅60–65 mm (from bottom to top)/∅110 mm | ∅20.8 mm (average)/∅36.6 mm |
| Area ratio between two ports and nozzle bore | 2.54 | |
| Ar gas injection | No gas | 10 mL/minute (0.06% volume fraction for clear visualization of mold flows) |

flow patterns were recorded with three video cameras to provide a NF end view, surface bottom view and wide face (WF) front view.

Computational Modeling — To quantify the flow pattern in the nozzle and mold with the +15° (up angle) and –15° (down angle) nozzle port cases, a three-dimensional (3D) finite-volume computational model was applied. The steady, incompressible, Reynolds Averaged Navier-Stokes (RANS) equations with the standard k-ε model have been solved with the commercial computational fluid dynamics (CFD) package program, ANSYS FLUENT to estimate the time-averaged turbulent flow in the nozzle and mold.

The model used a one-quarter domain (adopting 2-fold symmetry) and included the tundish bottom region, nozzle and mold, as shown in Fig. 4. The nozzle port in the domain was simplified to a rectangular shape, without the rounded corner. The SEN domain was connected with the mold domain and calculated together to obtain more accurate simulations of fluid flow in the mold.[11] Each case used a structured mesh of ~150,000 hexahedral cells. Constant velocity (0.000573 m/second) was fixed as the inlet condition at the sides of the cylinder representing part of the tundish bottom, along with $10^{-5}$ $m^2/second^2$ for turbulent kinetic energy and $10^{-5}$ $m^2/second^3$ for turbulent dissipation rate. The velocity was calculated according to the flowrate in the water model and the surface area of the cylindrical sides of the tundish bottom region. At the mold bottom, outlet boundary conditions of 0 Pa of gauge pressure, $10^{-5}$ $m^2/second^2$ for turbulent kinetic energy and $10^{-5}$ $m^2/second^3$ for dissipation rate were applied. The top surface of the mold was given by a stationary wall with 0 Pa shear stress components for free-slip boundary condition. For the two cases, convergence of solving the equations was defined when all scaled residuals were stably reduced below $10^{-4}$.

Figure 4

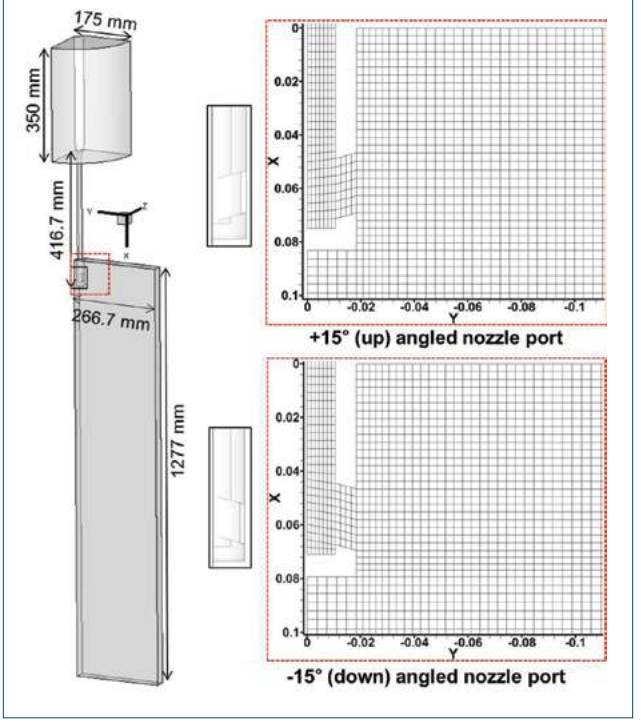


*Domain and mesh.*

## Figure 5

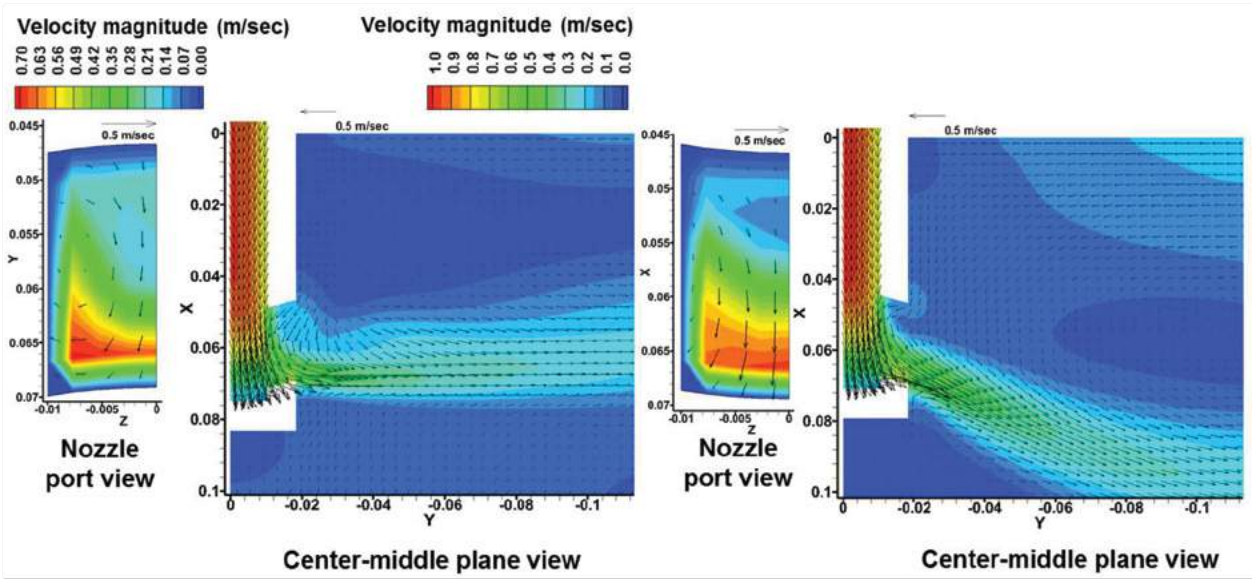


*Nozzle flow patterns with +15° (up angle) (a) and –15° (down angle) (b) nozzle port.*

## Figure 6

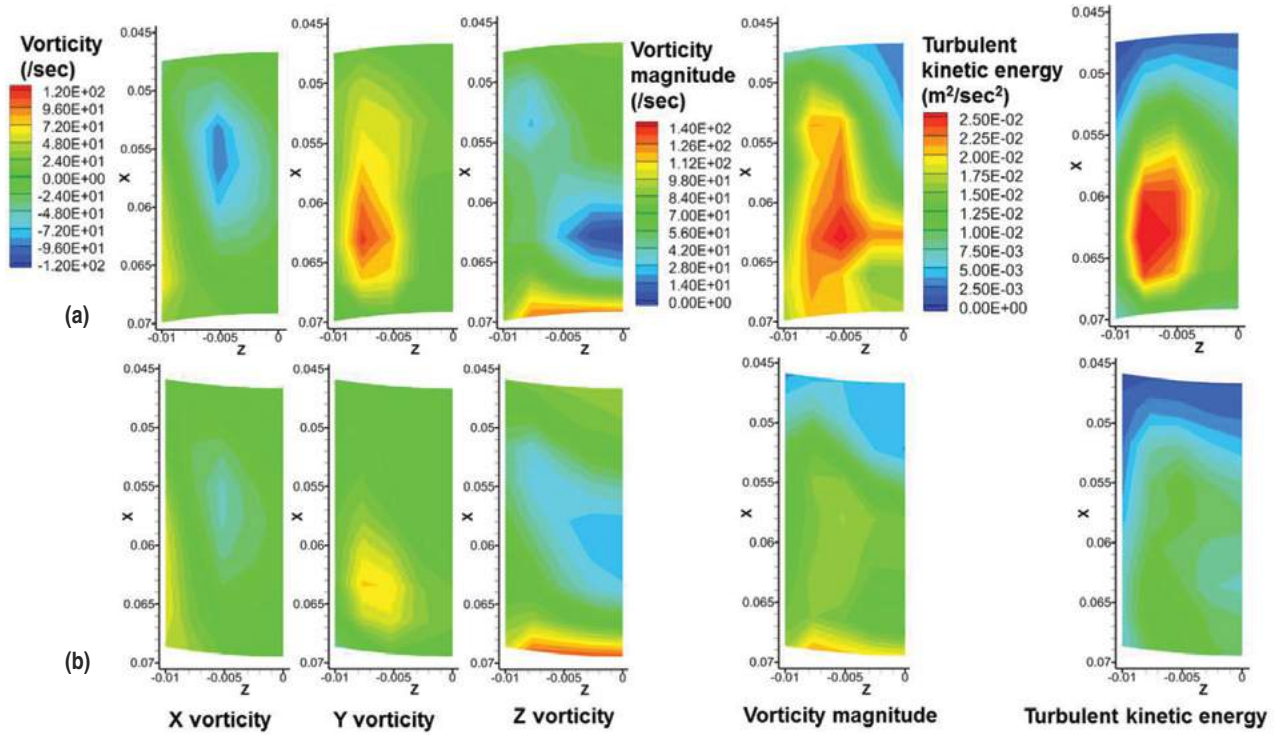


*Time-averaged vorticity components and turbulent kinetic energy at nozzle port exit with +15° (up angle) (a) and –15° (down angle) (b).*

## Nozzle Flow

To investigate the effect of nozzle port angle on nozzle flow pattern, velocity vectors with their magnitude contours are presented in Fig. 5 for the +15° (up angle) and –15° (down angle) port cases. Jet flow into the mold is deeper with the –15° (downward angled) port: the vertical jet angle in the casting direction is –19.3° with the –15° port and +1.12° with the +15° (up angle) port. At the nozzle port exit, the jet flow with +15° (upward angled) shows a larger flow-rotation region of swirl near the corner of the port sides.

For more detailed analysis of swirl with different nozzle port angles, vorticity components in each axis and turbulent kinetic energy of nozzle flow are given in Fig. 6. Vorticity vector, the curl of the velocity vector, describes the rotation of flow and is defined as follows:

$$\vec{\omega}_i = \nabla \times \vec{V}_i \qquad \text{(Eq. 3)}$$

where

$\vec{\omega}_i$ = vorticity,
$\nabla$ = gradient and
$\vec{V}_i$ = velocity in the three coordinate directions (x, y, and z).

The +15° (up angle) port produces higher vorticity components than the –15° (down angle) port does, especially y-vorticity. This produces higher vorticity magnitude and higher turbulent kinetic energy. The swirl rotation about the y-axis through the nozzle port contributes greatly to the flow fluctuations, resulting in ~2 times higher weighted-average turbulent kinetic energy: 0.0197 $m^2/second^2$ with the +15° (up angle) port and 0.0101 $m^2/second^2$ with the –15° (down angle) port. The predicted nozzle swirl phenomena are matched well with those observed in the water model experiments, as shown in Fig. 7. The measured swirl fills the entire port and alternates between clockwise and counterclockwise directions. Due to the quarter domain of the current computational model, the predicted swirl region area was smaller than the measured one. A transient model with no symmetry assumption would be needed for realistic capture of the transient swirl behavior in the nozzle.

Figure 7


*Transient swirl at nozzle port exit with +15° (up angle) in the one-third-scale water model: clockwise pattern (a) and counter-clockwise pattern (b).*

Further flow characteristics in the nozzle port exit are quantified with weighted-average calculations,[12] and given in Table 2. As expected, decreasing

Table 2

*Jet Characteristics*

| | +15° (up angle) | –15° (down angle) |
|---|---|---|
| Weighted-average x velocity (downward) (m/second) | –0.011 | 0.176 |
| Weighted-average y velocity (horizontal) (m/second) | –0.565 | –0.503 |
| Weighted-average z velocity (outward) (m/second) | –0.112 | –0.0638 |
| Vertical jet angle (degree) | +1.12 (toward surface) | –19.3 (toward mold exit) |
| Horizontal jet angle (degree) | –11.2 | –7.23 |
| Average jet speed (m/second) | 0.576 | 0.537 |
| Maximum velocity magnitude (m/second) | 0.838 | 0.711 |
| Weighted-average x vorticity (/second) | –7.41 | –1.18 |
| Weighted-average y vorticity (/second) | 43.0 | 27.1 |
| Weighted-average z vorticity (/second) | –5.57 | –20.8 |
| Weighted-average vorticity magnitude (/second) | 108 | 72.1 |
| Weighted-average turbulent kinetic energy($m^2/second^2$) | 0.0197 | 0.0101 |
| Weighted-average turbulent kinetic energy dissipation rate ($m^2/second^3$) | 0.669 | 0.269 |
| Backflow zone (%) | 28.2 | 27.9 |

nozzle port angle from +15° (up angle) to –15° (down angle), produces higher downward velocity with deeper vertical jet angle (directed more steeply downward). The horizontal jet angle becomes larger (directed more outward), and more toward the WF with higher outward velocity with the +15° (up angle) port. In addition, the increased nozzle swirl with the +15° (up angle) port causes: higher weighted average y vorticity, higher vorticity magnitude and higher turbulent kinetic energy. The size of the backflow region remains almost the same.

Figure 8

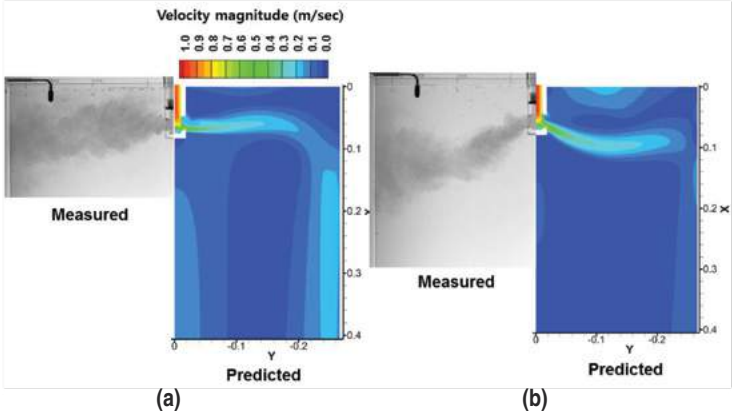


*Mold flow patterns with +15° (up angle) (a) and –15° (down angle) (b) nozzle port.*

## Mold Flow Patterns

Mold flow patterns predicted by the computational model for the two cases with different port angle are compared with those measured by dye injection in the one-third-scale water model in Fig. 8. The results using these two methods agree reasonably well. The +15° (up angle) port produces a shallower jet angle. On the other hand, jet flow becomes deeper and more stable with the –15° (down angle) port.

By comparing the dye diffusion areas in the visualized mold flow, jet wobbling phenomena were quantified and found to be more severe with the +15° (up angle) port. As shown in Fig. 9, this is due to the higher turbulent kinetic energy produced in the nozzle bottom, nozzle port and upper region of the mold with the +15° (up angle) port.

Figure 9

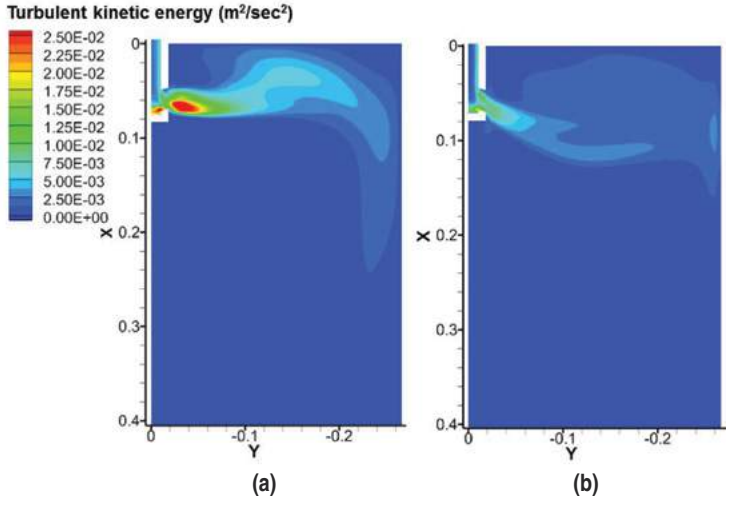


*Turbulent kinetic energy of mold flow with +15° (up angle) (a) and –15° (down angle) (b) nozzle port.*

Vertical velocity of the jet flow in the casting direction down the NF increases with increasing (more upward) jet angle, as shown in Fig. 10. Because the jet flow from the +15° (up angle) nozzle port impinges on the inside radius (IR) before reaching the NF as shown in Fig. 11, the jet flow loses its upward momentum and bends to flow more downward into the strand. On the other hand, the –15° (down angle) nozzle port produces a straighter jet flow directed toward the NF. The impingement angle on the NF is higher. Therefore, a higher momentum flow goes up the NF toward the surface, resulting higher surface velocity, as shown in Fig. 12b. However, surface velocity fluctuations are more severe with +15° (up angle) nozzle due to larger jet flow wobbling, as indicated by the higher turbulent kinetic energy in Fig. 12.

## Transient Surface Flow Velocity

For more detailed investigation of the influence of nozzle port angle on surface velocity, instantaneous surface velocities were measured using the electromagnetic current sensor. Two components of transient horizontal velocity (Vz: from inside radius to outside radius, Vy: from NF to SEN) were measured at three locations 10 mm below the surface during 1,000 seconds for both cases and are presented in Fig. 13. The average and standard deviation of each velocity component is given in Table 3.

Figure 10

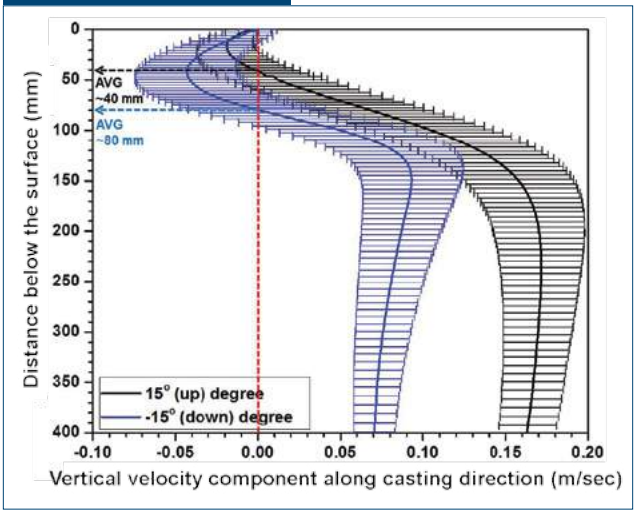


*Vertical velocity near narrow face, along casting direction.*

Horizontal velocity toward the SEN is higher than the other velocity component toward outside radius (OR), at all three locations for both cases. Thus, the flow is generally toward the SEN, as expected from the results of the predicted mold flow patterns. Surface flow becomes faster toward the SEN with both +15° (up angle) and –15° (down angle) nozzle ports. Decreasing the nozzle port angle from +15° (up angle) to –15° (down angle) makes the surface flow from the NF to the SEN faster and more stable. Surface flow with +15° (up angle) nozzle port is slower and less stable, showing larger fluctuations, especially near the SEN.

Average surface velocities toward the SEN in the centerplane, predicted by the RANS model, show good agreement with the measurements for both the +15° (up angle) and –15° (down angle) nozzle port cases. Although the trends are correct, the model

Figure 11

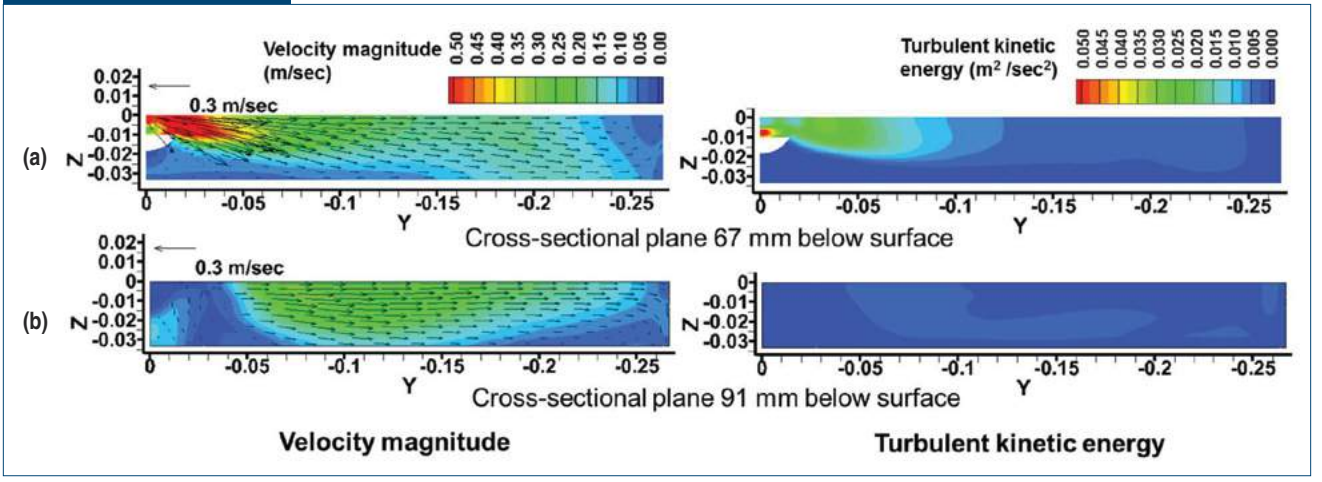


*Jet patterns at cross-sectional plane with +15° (up angle) (a) and –15° (down angle) (b) nozzle port.*

Figure 12

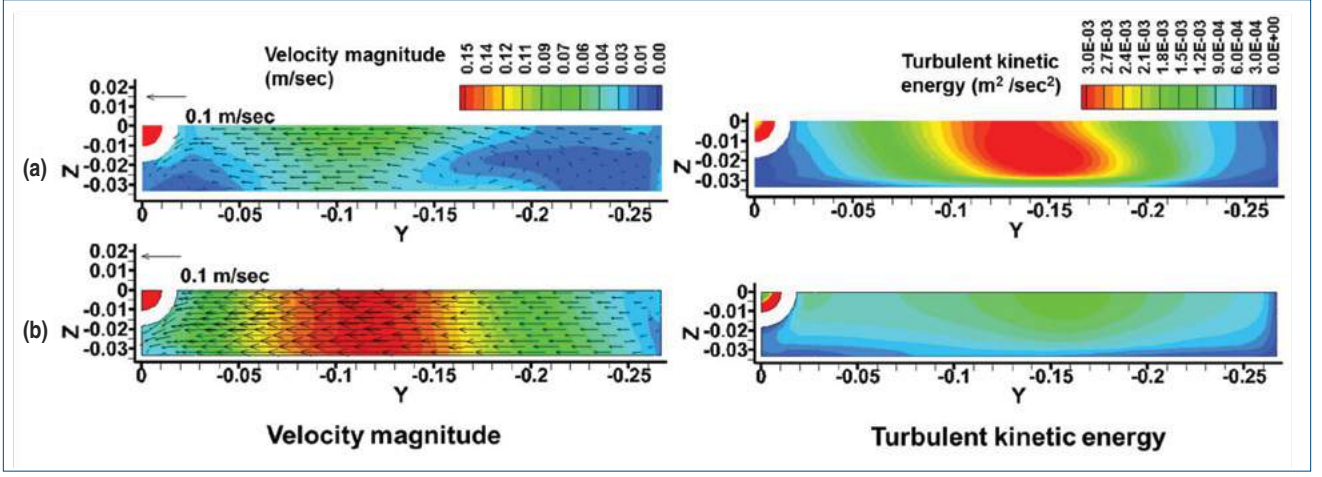


*Flow patterns at cross-sectional plane 10 mm below surface with +15° (up angle) (a) and –15° (down angle) (b) nozzle port.*

## Figure 13

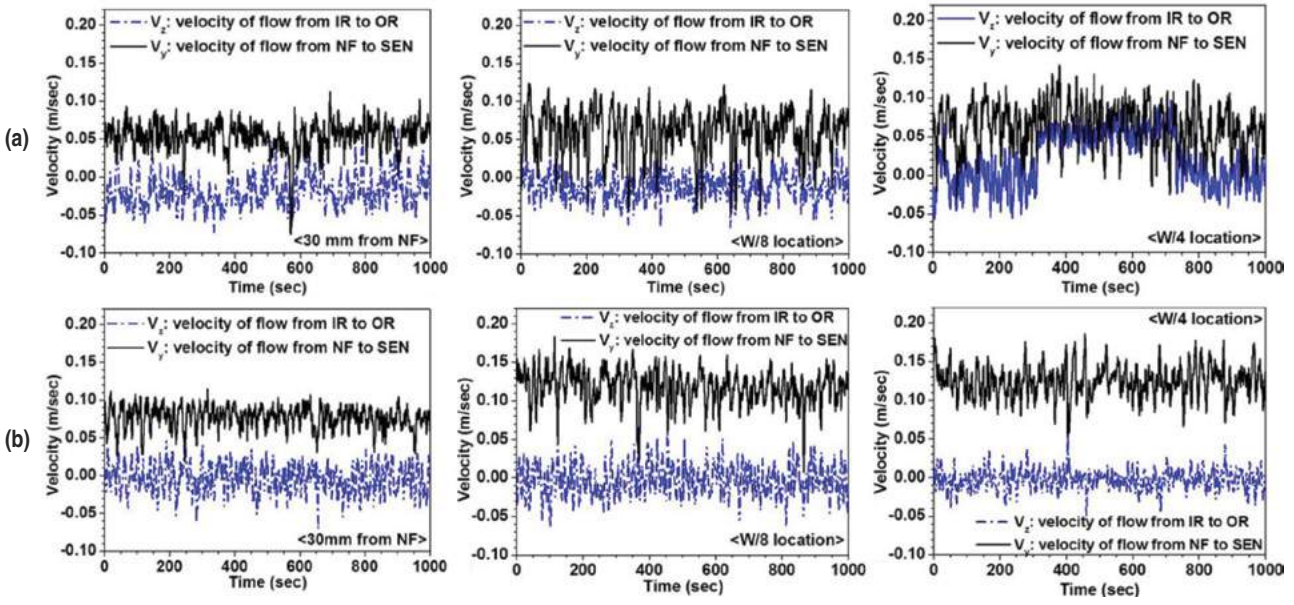


*Measured instantaneous surface velocity histories at the three different surface positions across the mold width with +15° (up angle) (a) and –15° (down angle) (b) nozzle port.*

## Table 3

*Measured Time-Averaged Velocity and Velocity Fluctuations*

| | | 30 mm from NF | W/8 location | W/4 location |
|---|---|---|---|---|
| +15° (up angle) | Velocity from NF to SEN | 0.0535 ± 0.0189 m/second | 0.0595 ± 0.0310 m/second | 0.0628 ± 0.0292 m/second |
| | Velocity from IR to OR | –0.0175 ± 0.0215 m/second | –0.0118 ± 0.0173 m/second | 0.0218 ± 0.0335 m/second |
| –15° (down angle) | Velocity from NF to SEN | 0.0768 ± 0.0144 m/second | 0.118 ± 0.0213 m/second | 0.124 ± 0.0199 m/second |
| | Velocity from IR to OR | –0.00381 ± 0.0190 m/second | –0.00266 ± 0.0204 m/second | –0.00278 ± 0.0126 m/second |

overpredicts the measured velocity fluctuations, likely due to the assumption of isotropic turbulence of the k-ε model, which is insufficient to capture the real anisotropic fluctuations. Transient models, such as large eddy simulation (LES), which can calculate more reasonable velocity fluctuations caused by anisotropic turbulence, are needed to improve the prediction of transient flow behavior, which is so important at the surface.

## Summary and Conclusions

Velocity measurements, die injection observations, and computational modeling with a standard k-ε RANS model were applied to investigate the effect of nozzle port angle on time-averaged flow and flow variations in a one-third-scale water model of the lower tundish, nozzle and mold during steady continuous slab casting of steel. Specifically, the effect of +15° (up

## Figure 14

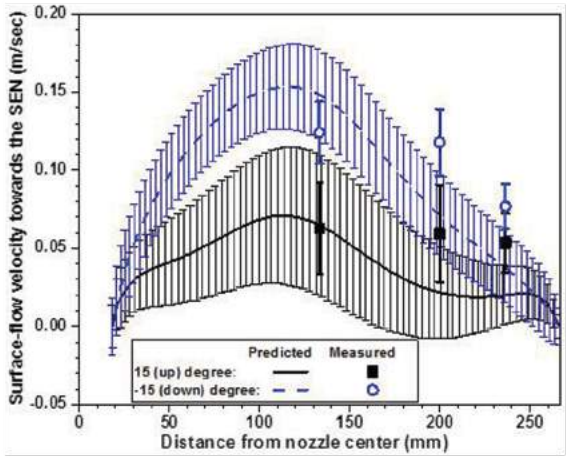


*Comparison of surface velocity toward the SEN between the measurements and the computational predictions.*

angle) and –15° (down angle) nozzle port were investigated in a typical bifurcated port SEN submerged 140 mm in a 200 mm (thickness) x 1,600 mm (width) strand casting at 0.8 m/minute.

- The RANS model prediction shows a very good quantitative match with mold flow patterns, average surface velocity profile and surface velocity fluctuations measured in the one-third-scale water model.
- Higher average surface velocity is produced with a port angle of –15° (down). Shallower port angle, +15° (up), has slower surface velocity. Thus, in general, increased surface velocity occurs when the jet impinges first on the NF at an upward angle. That means that surface velocity is slower if the jet impinges first on the WF or near the corner.
- Jet flow from the +15° (up) nozzle port produces stronger swirl with higher vorticity and turbulent kinetic energy, resulting in more severe wobbling in the mold than with –15° (down) ports; this up-angled jet sometimes impinges first on the top surface causing higher surface instability (low-frequency high-amplitude fluctuations), even though it has lower surface velocity, for these casting conditions.
- Unstable flow pattern results from the +15° (up) nozzle with the current casting conditions, oscillating between classic single- and double-roll flow patterns. This is likely because pressure sucks the jet up to impinge first on the top surface or down to impinge on the WF before going toward NF.
- Up-angled nozzles with non-optimal SEN depth could be detrimental in causing both severe surface instability (surface defects) and abnormal downward flow (internal defects) deep into the mold cavity.
- The surface flow instability could increase surface cracks, powder entrapment and associated downstream problems, especially in advanced high-strength steels.
- Deeper submergence is suggested for up-angled nozzle in this caster system to enable jet flow to impinge first on the NF.
- High-frequency low-amplitude turbulence without surface instability improves mixing, and heat transfer to the meniscus; casting conditions should be chosen to avoid high-power, lower-frequency oscillations.

## Acknowledgments

The authors thank POSCO and Shin-Eon Kang, POSCO Technical Research Laboratories, for providing the water model, and Hyun-Na Bae, Dae-Woo Yoon, and Seung-Ho Shin of POSTECH for help with the one-third-scale water model experiments. Support from the Continuous Casting Consortium at University of Illinois at Urbana-Champaign, the Continuous Casting Center at Colorado School of Mines, POSCO, South Korea (Grant No. 4.0011721.01) and the National Science Foundation (Grant Nos. 11-30882 and 15-63553) is gratefully acknowledged.

## References

1. T. Teshima, M. Osame, K. Okimoto and Y. Nimura, *Proceedings of 71 Steelmaking Conference,* Iron & Steel Society, 1988, pp. 111–118.
2. H. Nakamura, S. Kohira, J. Kubota, T. Kondo, M. Suzuki and Y. Shiratani, *Steelmaking Conference Proceedings,* Iron & Steel Society, 1992, pp. 409–415.
3. J. Kubota, K. Okimoto, A. Shirayama and H. Murakami, *Steelmaking Conference Proceedings,* Iron & Steel Society, 1991, pp. 233–241.
4. H.L.F. Von Helmholtz, *Monatsberichte der Koniglichen,* Vol. 23, 1868, pp. 215–228.
5. W. Thomson, *Philosophical Magazine,* Vol. 42, 1871, pp. 362–377.
6. T. Funada and D.D. Joseph, *J. Fluid,* Vol. 445, 2001, pp. 263–283.
7. J. Sengupta, B.G. Thomas, H. Shin, G. Lee and S. Kim, *Metall. Mater. Trans. A,* Vol. 37A, 2006, pp. 1597–1611.
8. H. Shin, S. Kim, B.G. Thomas, G. Lee, J. Park and J. Sengupta, *ISIJ Int.,* Vol. 46, 2006, pp. 1635–1644.
9. R. Chaudhary, G-G. Lee, B.G. Thomas and S-H. Kim, *Metall. Mater. Trans. B,* Vol. 39B, 2008, pp. 870–884.
10. F.M. Najjar, B.G. Thomas and Donald E. Hershey, *Metall. Mater. Trans. B,* Vol. 26B, 1995, pp. 749–765.
11. L. Zhang, Y. Wang and X. Zuo, *Metall. Mater. Trans. B,* Vol. 39B, 2008, pp. 534–550.
12. H. Bai and B.G. Thomas, *Metall. Mater. Trans. B,* Vol. 32B, 2001, pp. 253–267. ✦

AISTech This paper was presented at AISTech 2016 — The Iron & Steel Technology Conference and Exposition, Pittsburgh, Pa., USA, and published in the Conference Proceedings.